Proceedings of the 28th IEEE
EMBS Annual International Conference
New York City, USA, Aug 30-Sept 3, 2006

Measurement of safe thermal therapy levels: the case of ultrasonic waveguide interstitial applicator array

Boguslaw J. Jarosz

***Abstract*—This paper addresses the issue of heat toxicity using as an example heating with ultrasonic interstitial waveguide four-applicator array. We show that the experimental heating curves are closely followed by the ones from our FEA modeling using realistically shaped model. The thermal dose was calculated at locations considered to be at the border of the safe dose and compared to 20 CEM_{43} considered in literature as the safety threshold. We found some discrepancy between the two on comparison. In the paper, we propose an approach that leads to compromise between them; at the same time it helps to define the threshold temperature for each case.**

I. Introduction

Deposition of various forms of energy in tissues with the ultimate goal of thermal therapy has been used for a number of years [1]. In thermal therapy, the intended outcome is to heat (or cool) the tissue to high (or low) enough temperature for long enough time. This should lead to either immediate or delayed necrosis of the abnormal tissue ideally with sparing all the surrounding normal volume. Since variety of instrumentation has been proposed for that purpose, wide range of maximum temperatures and of heating time have been reported [2].

Relatively soon it has been concluded that higher the maximum temperature a shorter time is required to produce same biological effect and that led to the concept of the thermal dose [3]. The thermal dose has been used in evaluation of the therapeutic range of heating instrumentation [4 – 5]. Little attention has been given to use of the same concept to establish the range of heat toxicity of various devices. In that regard, a threshold temperature above which the tissue denaturation occurs was quoted. In [6] the authors decided to use one such threshold temperature for phantoms and another for tissue *in vivo*.

In this presentation we intend to address validity of the latter approach. We want to establish if the 'safe thermal dose' can be uniquely represented by some threshold temperature, the temperature above which properties of the normal tissue change. The concept of thermal dose applies to very many heating instrumentations that produce intermediate temperature elevation. That is one limitation of our discussion. Secondly, we intend to use experimental and

Manuscript received March 9, 2006. This work was supported in part by the National Research Council of Canada under Grant.

B. J. Jarosz is with the Ottawa-Carleton Institute for Physics, Ottawa, ON K1S 5B6 Canada (phone: 613-520-2600 x 4318; fax: 613-520-4061; e-mail: jarosz@ physics.carleton.ca).

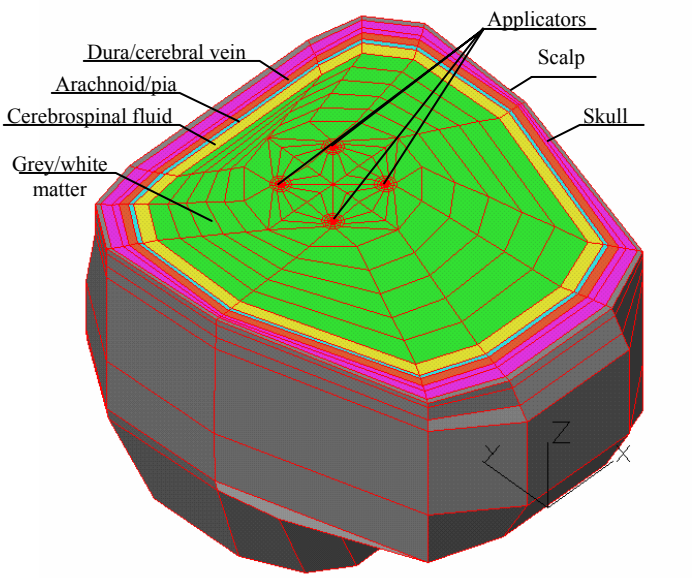

Figure 1 FEA full head 3-D model

FEA computation heating curves and those are instrumentation specific. In particular, the discussion applies to ultrasonic and microwave instrumentation with cylindrical symmetry of power deposition [5, 7–8]. It applies to heating with interstitial plate transducers [9] too if fast rotational scan is used.

II. Methodology

A. Heating curves

The heating curves in porcine muscle tissue were obtained with an ultrasonic interstitial waveguide applicator whose description was presented before [10]. Its crucial part is a cranial needle with its clad part serving as a waveguide and exposed to the tissue part, as an antenna. In the experiment, the antenna of 1.22-mm diameter was 1.5 cm long. The applicator was inserted into a slab of non-frozen muscle tissue of approximately 30 x 40 x 100 mm^3 in dimensions. Power ultrasonic transducer of the applicator was operated in cw mode at about 800 kHz from an HP3336C frequency synthesizer and 19 Vrms from an IFI-M50 radiofrequency power amplifier.

The temperature was determined with a 230-μm bead size and 50- μm wires Fenwal microthermistor at the tip of G-25 hypodermic needle. The needle was inserted into the tissue to a 2-mm radial distance from the antenna midway along the antenna's length. To read the temperature, the microthermistor was in a resistance bridge. Output of the

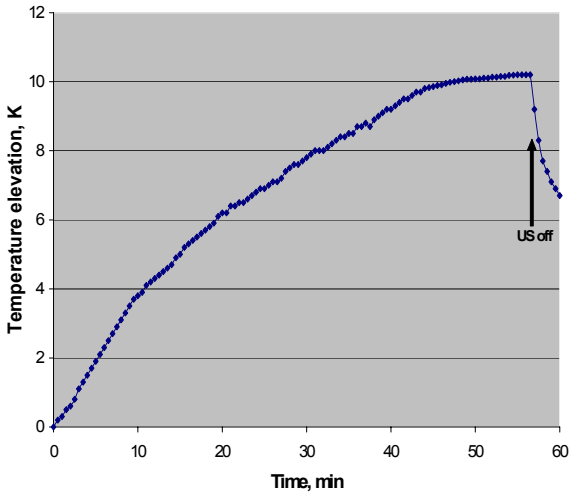

Figure 2 Heating curve in porcine muscle

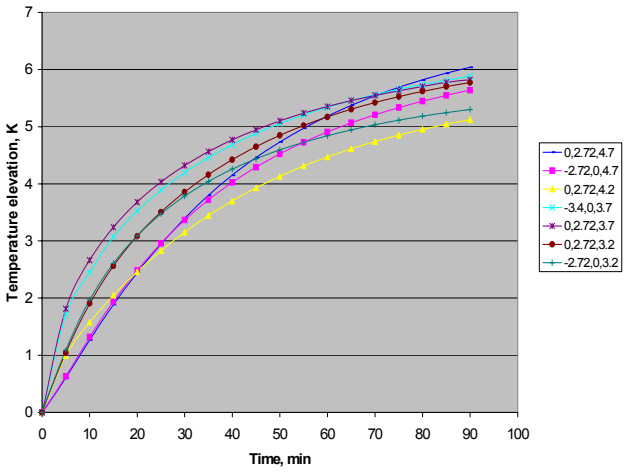

Figure 3 Heating curves from FEA computations

resistance bridge was connected to a 16-bit resolution DATASCAN data acquisition system. With the microthermistor in its resistance bridge, the system was calibrated against the reading of an YSI44201 thermilinear component in MATLAB environment. The readings of temperature in the tissue and outside room temperature were taken every half a minute.

B. FEA Computations

Full head model shown in Fig. 1 has been built as described in detail previously [5]. The model had several types of tissue labeled in Fig. 1. In computations, their respective physical properties [5] have been used. It was assumed that the heating is produced with an array of four ultrasonic interstitial applicators shown in Fig. 1 as dark circular circles. Their antennas were 3.2 – 4.7 cm below the scalp. Transient analysis of the bioheat transfer equation in FEA approach was used to obtain heating curves for various locations. Temperature–time dependence from these curves was the basis of thermal dose computations. The dose is expressed in terms cumulative equivalent minutes of maintaining the tissue at 43^0C. Its analytical form may be written as [3]:

$$CEM_{43} = \begin{cases} 0, T < 39^0 C \\ \int R^{43-T} dt, T > 39^0 C \end{cases}. \qquad (1)$$

In equation (1), T is the temperature, t – time and $R = 0.25$ below 43^0C and = 0.5 above 43^0C. Since there is no straightforward analytical expression for $T(t)$, the integration in dose calculations has been done numerically.

III. Results

Fig. 2 shows a typical heating curve obtained with our waveguide applicator. Similar heating curves are obtained with other interstitial instrumentation. The main difference between the curves is initial rate of heating in reaching the final desired temperature. This is also true if an array of applicators is used. Fig. 3 shows heating curves obtained in our FEA computations at various locations in the head model. These locations were chosen to correspond to the non-toxicity range of the thermal treatment based on previously assumed threshold toxicity temperature of about 42.5^0C, *i.e.*, 5.5 K temperature elevation. The figure legend gives coordinates of the location using the coordinate system shown in Fig. 1.

The results of Fig. 3 are critically evaluated in Figs. 4 and 5 that show calculations of the actual dose. The two figures were obtained for temperature at the scalp of 18 and 0^0C, respectively, *i.e.*, when cooling at the head surface accompanies heating with the applicator array. Following [11], we took 20 CEM_{43} as a limit for no substantial damage in brain tissue. The dose was calculated after 87 min of heating and the temperature at that time was obtained from the data that was used to produce Fig. 3 and may be used to produce similar figure with 0^0C at the scalp. They show that while in some cases the assumption of 42.5^0C as a safe limit is an exaggeration on a too much caution (Fig. 4), in others (Fig. 5) it is a very good measure of instrumentation safety. The latter figure implies that if measured temperature is below 42.5^0C, we determined safe limit of the instrumentation. However, Fig. 4 suggests that bearing in mind determination error (vertical bars), 43^0C should be considered as that limit.

In experimental practice it may be quite inconvenient to do the dose calculation. Conclusion about a threshold temperature becomes of paramount importance in verification of the safe limits. With inconclusive results from the two last computations we decided to look into the issue in case of external temperature held at 47^0C, *i.e.*, with external heating at the scalp during the thermal therapy session. Fig. 6 gives the thermal dose and temperature at the nodes that were at the boundary of 'heat toxicity' as described above. The figure demonstrates that at specific locations the thermal dose exceeds 20 CEM_{43} well below 42.5^0C. Yet, at many locations the temperature above 43^0C does not result in exceeding the safe dose. The curve in Fig.

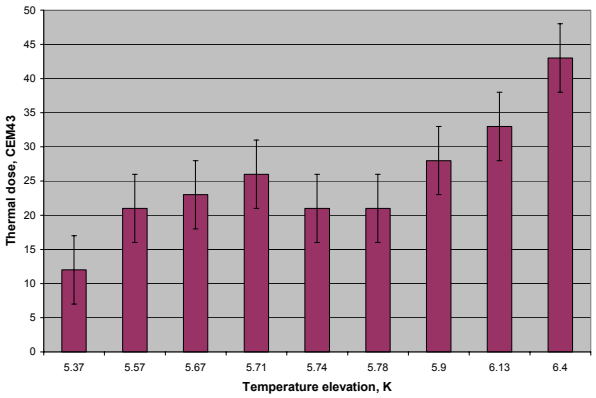

Figure 4 Thermal dose vs. temperature elevation with external temperature of 18^0C

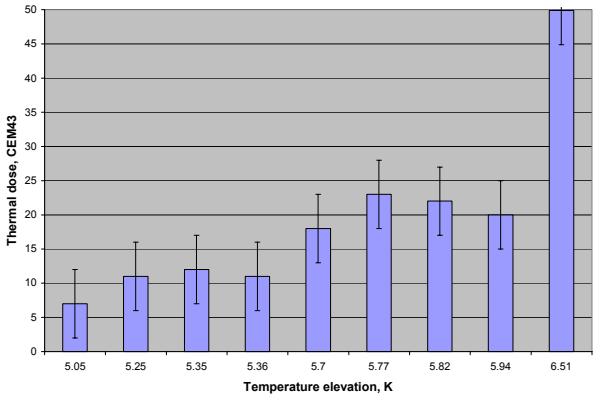

Figure 5 Thermal dose vs. temperature elevation with external temperature of 0^0C

6 being polynomial fit of the data shows dose trend vs. temperature. We think that the temperature where the curve intersects 20 CEM_{43} may be taken as a safety threshold.

IV. Discussion

Figs. 2 and 3 illustrate the importance of FEA modeling in obtaining detailed temperature pattern practically not available from measurements. The curves in Fig. 3 are similar in shape to those in Fig. 2 as required. They were obtained for nodes with approximately same distance from the centre of the four-applicator array. Yet dynamics of temperature rise in time is very different depending on position of the node with respect to the outside of the model. To obtain similar experimental curves, a substantial number of temperature sensors would have to be inserted and then one expects significant modification of physical properties by such insertion.

The various curves of Fig. 3 correspond to locations where heat toxicity may be of concern. The range within which maximum temperature elevation is observed is relatively narrow, slightly less than 1 K and about 15% of the average temperature elevation. Despite the variation in the maximum temperature, the thermal dose was even in narrower range, very close to 20 CEM_{43}. Obviously on integration suggested by (1) not only the maximum temperature, but also initial heating rate is crucial.

The depth of the nodes for which the curves were produced varies from 3.2 to 4.7 cm (the z-coordinate of Fig. 1), *i.e.*, it corresponds to the length over which US has been deposited in the tissue. The location of the nodes is symmetrical with respect to the centre of the array. As it is clearly seen, the symmetry in location does not find a reflection in symmetry of temperature distribution. For example, consider the nodes at 3.2 at 4.7 cm depth at 2.72 cm to the right of the array center (along the y-axis shown in Fig. 1) depicted in Fig. 3 as a dark curve with small rectangles representing the read out points and another dark curve with solid circles for the points. While the first curve reaches higher temperature, its initial rise is much slower. As a result, the thermal dose at the two locations is very similar.

An analysis of two dark curves shown in Fig. 3 with points represented by crosses and solid circles for the nodes at the same depth of 3.2 cm explains why we expect similar thermal doses despite a difference in detailed shape of the curves. Since the Dewey-Sapareto formalism involves exponential dependence of the dose on temperature, the fact that the curves with crosses has initially slightly higher rate of heating makes up for slightly lower temperature at the plateau.

It is also interesting to note that the simulations show an 'inversion' in the temperature pattern inside the model. That is demonstrated by the fact that both the curves for locations 3.7 cm deep have higher temperature than those 4.2 and 3.2 cm deep. This comes from the fact that modeled head has highly asymmetrical shape. It also points out that the caution must be exercised when using simplified models of the head [12] in calculations of other effects in the brain. In our case, the inversion referred to above is a direct consequence of external temperature fixed at 18^0C. It is a clear demonstration that the heating effects are enormously influenced by external conditions, but again these effects are noticeable if a realistic shape model is used.

The need for using realistically shaped organ in simulation is further amplified in Figs. 4 and 5. On comparison of results presented there one sees clearly that the thermal dose at a given location is strongly influenced by the external temperature. This influence may seem surprising at first glance, as, on average, with 0^0C at the scalp the 20 CEM_{43} occurs at lower temperatures compared with those when the temperature at the scalp of 18^0C. Closer analysis indicates that in the case of low external temperature there must be a multidirectional heat flux to maintain basal temperature inside the head and in some places the flux is superimposed on a local heating by the array. Fig. 6 further corroborates the above interpretation. The results in the figure obtained for 47^0C at the scalp show that there is no simple relationship between the temperature

reached at the end of heating session. It may be seen from the figure that 20 CEM_{43} dose is exceeded even though the temperature is as low as 42.2^0C. This toxicity limit is significantly surpassed at about 42.6-42.8^{0}C and 43.1^{0}C in some locations. While an excessive dose at the former low temperature looks as exception from the general trend (only a single dose within the experimental error is above the 20 CEM_{43} line), the latter group is represented by far more locations that above the line. Note that there is a group of locations with temperature in the 43.0-43.1^{0}C range with the dose below the limit. Since Fig. 6 presents results at 41 locations in the head as opposed to nine locations of Figs. 4 and 5, we used statistical analysis of the former. The curve shown in the figure represents a spline fit of the data, thus representing a general trend of the 20 CEM_{43} dose *vs*. temperature. The fit demonstrates that the curve intersects the 20 CEM_{43} line at about 42.6^0C. We propose that the latter temperature be used in this particular case as the determination of the heat toxicity range. This is not a generally valid determination. It is thought that every time there is a need to judge heat toxicity from a temperature pattern, similar evaluation to suggested in Fig. 6 is done, *i.e*., intersection of the statistical fit curve with the organ heat toxicity threshold indicates the temperature at which statistically one would expect the toxicity.

The above interpretation points out to possibility of practical fast evaluation of toxicity risks. It is based on the current Sapareto-Dewey method of thermal dose calculations. On inspection of Figs. 4 – 6 it is evident that there is a need for development of alternative definition of thermal dose. In particular, both Figs. 4 and 6 have location with temperature above 43^0C where the dose is still below the chosen toxicity threshold. Yet, quite often hyperthermia treatments use that temperature as a measure of the therapy success [13]. It seems that the current dose calculations attach too much emphasis to temperature rise (the temperature being in the exponent) and not enough account for the maximum temperature. We intend to revisit this particular issue in future simulations of thermal therapy and in measurements carried out in geometry mimicking that of the real organ.

V. Conclusions

Our FEA 3-D modeling with realistically shaped organ show details of temperature pattern which are hardly achievable from experiments. The details led to some surprising results when external temperature was varied. They are only available if the FEA model resembles closely the organ (head in our case) as simplified geometry utilizing symmetries may occlude some effects. For example, we observed an 'inversion' in temperature at some depth when the external temperature varied from 0 to 18 to 47^0C.

With enough data points we were able to propose statistical reference to the safety limit when comparing the thermal dose and temperature. Our results show that the currently used methodology for dose calculations must be revisited.

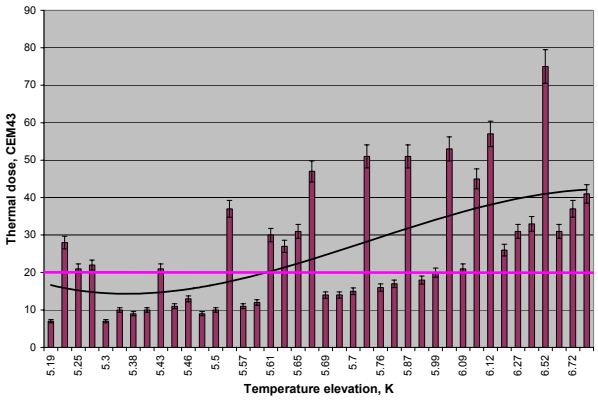

Figure 6 Thermal dose vs. temperature elevation at external temperature of 47^0C

Acknowledgment

The author wishes to acknowledge contribution of Sara St. James to experimental measurements of the array heating in tissue.

References

[1] M.H. Seegenschmiedt and R. Sauer, Eds., *Interstitial and Intracavitary Thermoradiotherapy*, Springer-Verlag, Heidelberg, 1993.

[2] P.R. Stauffer *et al.*, "Introduction: Thermal ablation therapy", *Int. J. Hyperthermia*, vol. 20, pp. 671-677, 2004.

[3] S.A. Sapareto and W.C. Dewey, "Thermal dose determination in cancer therapy", *Int. J. Radiat. Oncol. Biol. Phys.*, vol. 10, pp.787-800, 1984.

[4] C.J. Diederich *et al.*, "Transurethral ultrasound applicators with directional heating patterns for prostate thermal therapy: In vivo evaluation using MR thermometry", *Med. Phys*., vol. 31, pp. 405-23, 2004.

[5] B.J. Jarosz, "External Temperature Effects on Therapeutic Heating with Interstitial Instrumentation", *submitted.*

[6]] D. Arora *et al.*, " Direct thermal dose control of constrained focused ultrasound treatments: phantom and *in vivo* evaluation", *Phys. Med. Biol*., vol. 50, 1919–1935, 2005.

[7] R.D. Novels *et al.*, "Microwave catheter design", *IEEE Trans. Biomed. Eng.*, vol. 45, pp.885-890, 1998.

[8] D.L. Deardorf *et al.*, "Air-cooling of direct-coupled applicators for interstitial hyperthermia and thermal coagulation", *Med. Phys.*, vol. 25, pp. 2400-9, 1998.

[9] R. Chopra *et al.*, "Multifrequency ultrasound transducers for conformal interstitial thermal therapy", *IEEE Trans. Ultrason. Freq. Contr. Ferroelectrics*, vol. 50, pp. 881-887, 2003.

[10] B.J. Jarosz and S. St.James, "Integrated Temperature Sensor for Determination of Ultrasound Interstitial Applicator Heating Effects ", *IEEE Trans. Instrum. Meas.* , vol. 54, pp. 1171-1174, 2005.

[11] M.W. Dewhirst *et al*, "Basic principles of thermal dosimetry and thermal thresholds for tissue damage from hyperthermia", *Int. J. Hyperthermia*, vol. 19, pp.267-294, 2003.

[12] K.R.Dewey, M. Riehl, "Suppressing the surface field during transcranial magnetic stimulation", *IEEE Trans. Biomed. Eng.*, vol. 53, pp. 190-4, 2006.

[13] L. Roizin-Towle *et al*., "The response of human and rodent cells to hyperthermia", *Int.J. Radiation Oncology Biol. Phys*., vol. 20, pp. 751-756, 1991.